Terr. Atmos. Ocean. Sci., Vol. 23, No. 3, 303-316, June 2012 doi: 10.3319/TAO.2011.11.23.01(A)

Contrasting Various Metrics for Measuring Tropical Cyclone Activity

Jia-Yuh Yu[1, 2, *] and Ping-Gin Chiu[2]

[1] *Department of Atmospheric Sciences, Chinese Culture University, Taipei, Taiwan*
[2] *Graduate Institute of Earth Science, Chinese Culture University, Taipei, Taiwan*

Received 31 December 2010, accepted 23 November 2011

ABSTRACT

Popular metrics used for measuring the tropical cyclone (TC) activity, including NTC (number of tropical cyclones), TCD (tropical cyclone days), ACE (accumulated cyclone energy), PDI (power dissipation index), along with two newly proposed indices: RACE (revised accumulated cyclone energy) and RPDI (revised power dissipation index), are compared using the JTWC (Joint Typhoon Warning Center) best-track data of TC over the western North Pacific basin. Our study shows that, while the above metrics have demonstrated various degrees of discrepancies, but in practical terms, they are all able to produce meaningful temporal and spatial changes in response to climate variability. Compared with the conventional ACE and PDI, RACE and RPDI seem to provide a more precise estimate of the total TC activity, especially in projecting the upswing trend of TC activity over the past few decades, simply because of a better approach in estimating TC wind energy. However, we would argue that there is still no need to find a "universal" or "best" metric for TC activity because different metrics are designed to stratify different aspects of TC activity, and whether the selected metric is appropriate or not should be determined solely by the purpose of study. Except for magnitude difference, the analysis results seem insensitive to the choice of the best-track datasets.

Key words: Tropical cyclone activity, Climate variability, Modified Rankine vortex

Citation: Yu, J. Y. and P. G. Chiu, 2012: Contrasting various metrics for measuring tropical cyclone activity. Terr. Atmos. Ocean. Sci., 23, 303-316, doi: 10.3319/TAO.2011.11.23.01(A)

1. INTRODUCTION

Tropical cyclones (TCs) are among the most devastating weather systems on Earth because of the vast size of extreme wind and precipitation. Each year, about 88 TC systems reaching tropical storm intensity (> 34 knots) form around the globe, with nearly a quarter ever growing into the severe hurricane intensity (> 95 knots) (Henderson-Sellers et al. 1998; Bell et al. 2000). Observations have shown that, while the annual number of TC formation is relatively stable on a global scale (Emanuel 2005; Webster et al. 2005), its year-to-year variability on a regional scale, nonetheless, can be very significant under the influence of regional climate variability, such as El Niño/Southern Oscillation (Chan 2000; Wang and Chan 2002; Wu et al. 2004; Camargo and Sobel 2005), Pacific Decadal Oscillation (Saunders and Harris 1997; Goldenberg et al. 2001; Yumoto and Matsuura 2001; Ho et al. 2004), and global warming (Sugi et al. 2002; Knutson and Tuleya 2004; Emanuel 2005; Webster et al. 2005; Holland and Webster 2007). Therefore, understanding how TC activity is physically controlled by various climate phenomena is of crucial importance if one expects to obtain a skillful seasonal TC activity forecast. To achieve this goal, choosing a metric that can properly represent the overall magnitude of TC activity (i.e., total TC activity) is highly desirable.

Among various metrics commonly used for measuring the total TC activity, the "number of tropical cyclones" (hereafter NTC) is perhaps the most popular due to its easy-to-interpret nature (Landsea et al. 1996; Chen et al. 1998; Goldenberg et al. 2001; Emanuel 2006). Since NTC only considers the total number of TC formations in an ocean basin, the contribution from intensity and duration of a TC is by no means included. Therefore, "tropical cyclone days" (hereafter TCD) is often used as an auxiliary of NTC by accumulating durations of all TC records in an ocean basin (Wang and Chan 2002; Emanuel 2005). In calculating TCD,

* *Corresponding author*
E-mail: jiayuh@atmos.pccu.edu.tw

each TC record accounts for a duration period of 6 hours. Since a stronger TC system also tends to last longer than a weaker one (Camargo and Sobel 2005; Chen et al. 2006), the contribution from TC intensity is implicitly included in TCD as well.

Recently, the "accumulated cyclone energy" (hereafter ACE) index proposed by NOAA (National Oceanic and Atmospheric Administration) has been used by several hurricane operational centers (or research institutes) as an alternative measure of the total TC activity. The ACE index explicitly includes the contribution from intensity and duration of a TC by annually accumulating the 6-hourly wind energy of all TC records in an ocean basin. In calculating ACE, the wind energy associated with a TC is evaluated at the radius of maximum wind, which is assumed to be equivalent to the square of the maximum wind speed (Bell et al. 2000; Waple et al. 2002). Since the radial wind structure in a TC varies substantially depending on the strength (Weatherford and Gray 1988a, b; Mallen et al. 2005), such a simple approximation may lead to a spurious estimation of the total TC activity. To remedy this defect, Yu et al. (2009) proposed a revised version of ACE. Instead of estimating the wind energy at the radius of maximum wind as in ACE, the revised accumulated cyclone energy (hereafter RACE) index considers the mean wind energy averaged over a modified Rankine vortex structure.

Moreover, Emanuel (2005) proposed a new approach to measure the total TC activity based on the total dissipation of wind power, and a simplified power dissipation index (hereafter PDI) was introduced accordingly. Similar to the ACE index, the PDI is defined by annually integrating the cubic of the maximum wind speed over the period containing TC records. It was shown that the variability of PDI on time scales of a few years and more was strongly correlated with sea surface temperature (SST), in particular, over the tropical Atlantic Ocean (Emanuel 2007).

While most studies have shown a robust relationship between seasonal TC activity and regional climate variability, they sometimes concluded magnitude changes of TC activity in a rather diverse range. For instance, by analyzing the occurrence frequency of intense hurricanes over the Atlantic Ocean, Landsea et al. (1996) found a downward trend of TC activity during the period 1950 ~ 1995. In contrast, by analyzing the time series of PDI, Emanuel (2005) found an upward trend of TC activity roughly over the same period. This disagreement suggests that we lack a firm understanding of how these metrics behave quantitatively in response to both regular and irregular climate variations.

In this study, differences among various metrics are compared using the best-track data of TC over the western North Pacific (WNP) basin. In section 2, the data and analysis methods are introduced. Section 3 compares the differences in annual cycle and spatial distribution patterns. Section 4 compares the anomalous patterns of TC activity associated with El Niño and La Niña events, along with a comparison of long-term TC activity trends over the past few decades. Conclusion and discussion are presented in section 5.

2. DATA AND METHODS

The best-track data of TC records achieved in the Joint Typhoon Warning Center (JTWC) is employed to contrast the differences among various metrics used for measuring the TC activity. This JTWC best-track data contains location and intensity of each TC system occurring over the WNP, with a 6-hourly resolution from 1949 to the present. Since satellite monitoring of TC systems was not available prior to 1965, unless otherwise mentioned, only the TC records reaching at least tropical storm intensity (≥ 35 knots) during the period 1965 ~ 2008 are analyzed in this study. Because definitions of NTC and TCD (in units of days) are quite straightforward, we discount their discussions here for brevity.

The ACE index, first documented in Bell et al. (2000) in an attempt to provide a quantitative measure of the total TC activity, is defined by accumulating the 6-hourly wind energy of all TC records in an ocean basin annually. In calculating ACE, the cyclone wind energy is evaluated at the radius of maximum wind, which is simply assumed to be equivalent to the square of the maximum wind speed (Waple et al. 2002):

$$ACE = \sum v_{\max}^2 \tag{1}$$

where $v_{\max}$ denotes the maximum sustained wind speed typically measured at a height of 10 m over a given period of time. The period used to estimate $v_{\max}$ varies depending on meteorological agencies. In JTWC data, $v_{\max}$ is defined by averaging the winds over a period of one minute.

Instead of characterizing wind energy at the radius of maximum wind as in ACE, the RACE index considers a more precise estimate of wind energy by taking an area mean of Eq. (1) over a modified Rankine vortex wind structure such that contributions to TC activity from various TC strengths can be fairly included (Yu et al. 2009). This gives

$$RACE = \frac{1}{\tilde{r}_c^2}\left[\frac{1}{2} + \frac{\tilde{r}_c^{(2-2\alpha)} - 1}{(1-\alpha)}\right]\sum v_{\max}^2 \tag{2}$$

where $\tilde{r}_c$ denotes the cut-off radius (unitless) within which the wind energy is measured and α depicts the decaying tendency of wind beyond the radius of maximum wind. Based on the same JTWC data, Yu et al. (2009) suggested that the best-fit value for α is 0.51. Both ACE and RACE are in units of 10^4 knots^2.

Similar to ACE, the PDI defined by Emanuel (2005) can be obtained by integrating the cubic of the 6-hourly maximum wind of all TC records in an ocean basin annually, which gives

$$PDI = \int_0^{\tau} v_{\max}^3 d\tau \tag{3}$$

where $v_{\max}$ denotes the maximum sustained wind speed and τ represents the total duration (in units of second) containing TC records.

As in RACE, we again consider a revised version of PDI by taking an area mean of Eq. (3) over a modified Rankine vortex wind structure, which yields

$$RPDI = \frac{1}{\tilde{r}_c^2}\left[\frac{2}{5} + \frac{2\tilde{r}_c^{(2-3\alpha)} - 2}{(2-3\alpha)}\right]\sum v_{\max}^3 \tag{4}$$

Note that the notations used in Eq. (4) are identical to those in Eq. (2) and we should refer to this version as the "revised power dissipation index" (hereafter RPDI). A detailed derivation of Eq. (4) is also presented in Appendix A for reference. To obtain a manageable number, both PDI and RPDI are in units of 10^9 m^3 s^{-2}.

3. CONTRAST IN CLIMATOLOGY

In this section, climatic features of NTC, TCD, ACE, RACE, PDI and RPDI are compared, with a focus on their annual cycles and spatial distribution patterns. To highlight the differences, results from both monthly and pentadly temporal resolutions are presented.

3.1 Seasonal Cycle

Figure 1 first shows the monthly annual cycles of NTC, TCD, ACE, RACE, PDI and RPDI. On average, approximately 27 TCs occur each year over the WNP, with an annual TCD value of about 144 days, an ACE index of about 303, an RACE index of about 97, and the annual sizes of PDI and RPDI are about 786 and 129, respectively. At first glance, except for magnitude differences, these metrics seem to show a similar seasonal transition pattern, characterized by a period of frequent TC activity from July to November (JASON) and a period of relatively infrequent TC activity from December to the following June. Because over 75% of the annual TC activity occurs over JASON, this period is often referred to as the TC season of WNP (Ho et al. 2004).

Despite the seemingly high degree of similarity, some differences are still noted. As shown in NTC (see Fig. 1a), August stands out above the rest as the peak month for TC activity, followed by September, July, and October. For the remaining metrics (e.g., TCD, ACE, RACE, PDI and RPDI shown in Figs. 1b ~ f), nonetheless, September becomes the most frequent month for TC activity instead of August. Such a difference can be attributed to the inclusion of TC intensity and duration within these metrics. Moreover, the second peak month also differs among ACE, PDI, TCD, RACE and RPDI. For example, larger magnitudes of ACE and PDI tend to occur in the later period of JASON (e.g., October and November); while larger magnitudes of TCD, RACE and RPDI incline to appear in the earlier period (e.g., August and July). Because ACE and PDI both use the maximum sustained wind speed to characterize the wind power of TC, which has been shown to put additional weight on strong TC systems (Yu et al. 2009), it is speculated that more frequent occurrences of stronger TC systems in the later period of JASON are responsible for such a difference.

To elaborate, Fig. 2 shows the annual cycle of RACE/ACE ratio. Of particular interest are the lower RACE/ACE ratios occurring in October and November than those in July

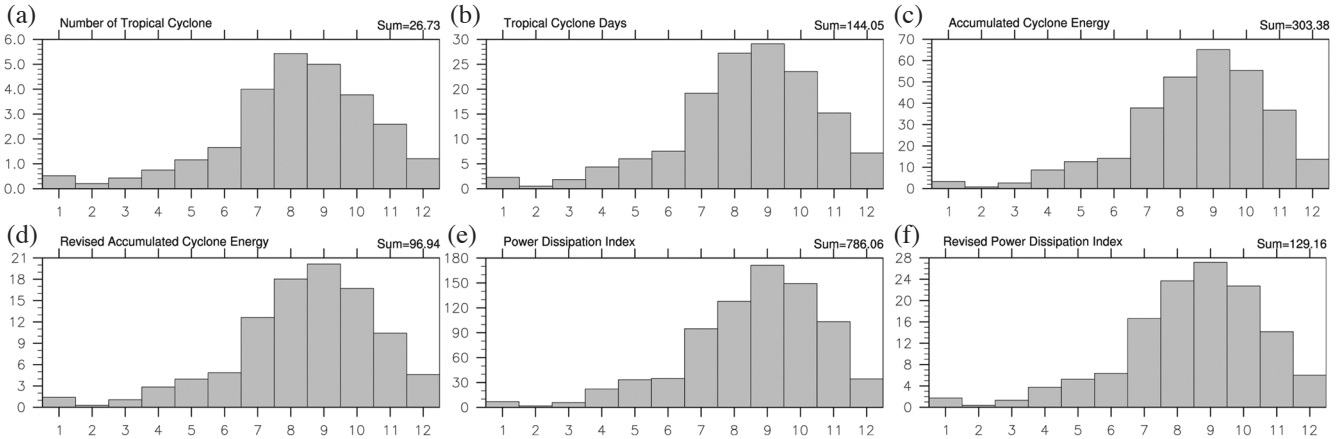

Fig. 1. Histograms showing the monthly annual cycle of TC activity over the entire WNP basin as measured by (a) NTC, (b) TCD (in units of days), (c) ACE (in units of 10^4 $knot^2$), (d) RACE (in units of 10^4 $knot^2$), (e) PDI (in units of 10^9 m^3 s^{-2}), and (f) RPDI (in units of 10^9 m^3 s^{-2}), respectively, over the period 1965 ~ 2008. Annual-mean magnitudes of the respective metrics are displayed at the upper right corners.

and August. Since a lower RACE/ACE ratio month generally denotes the dominance of stronger TC systems (Yu et al. 2009), it shows that TC systems occurring in the later period of JASON are indeed frequently stronger than those occurring in the earlier period, concurring with the results shown in Fig. 1.

To highlight the relative contributions to TC activity from various intensities, we separate all TC systems into three groups, i.e., namely "tropical storm" ($34 < v_{max} \leq 63$ knots), "hurricane" ($64 \leq v_{max} \leq 95$ knots), and "severe hurricane" ($v_{max} > 95$ knots), respectively. To offer a more precise picture, the entire annual cycle is displayed in pentad resolution here. Note that such a manner allows us to distinguish the embedded high-frequency fluctuations from the slowly evolving monthly seasonal cycles. As shown in Fig. 3, pentads 36 to 66 (corresponding roughly to the period of JASON) stand out as the most frequent period for TC activity, consistent with the monthly annual cycle patterns shown in Fig. 1. Aside from the slowly evolving seasonal signals, fluctuations of shorter timescales emerge in all six metrics. It should be noted that while these fluctuations have timescales lying between 30 ~ 60 days, they do not directly imply influence of TC activity by the tropical intra-seasonal oscillation (TISO) because the observed TISO phases are loosely locked on the annual cycle (Matthews 2000). The results shown in Fig. 3 simply demonstrate the

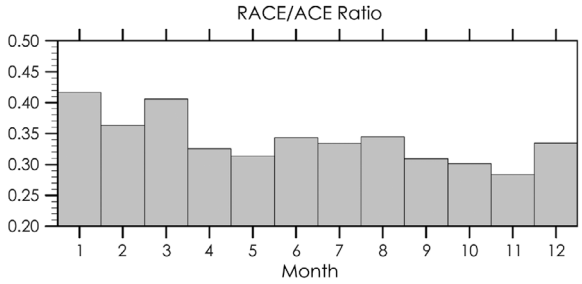

Fig. 2. Histograms showing the annual cycle of the RACE/ACE ratio.

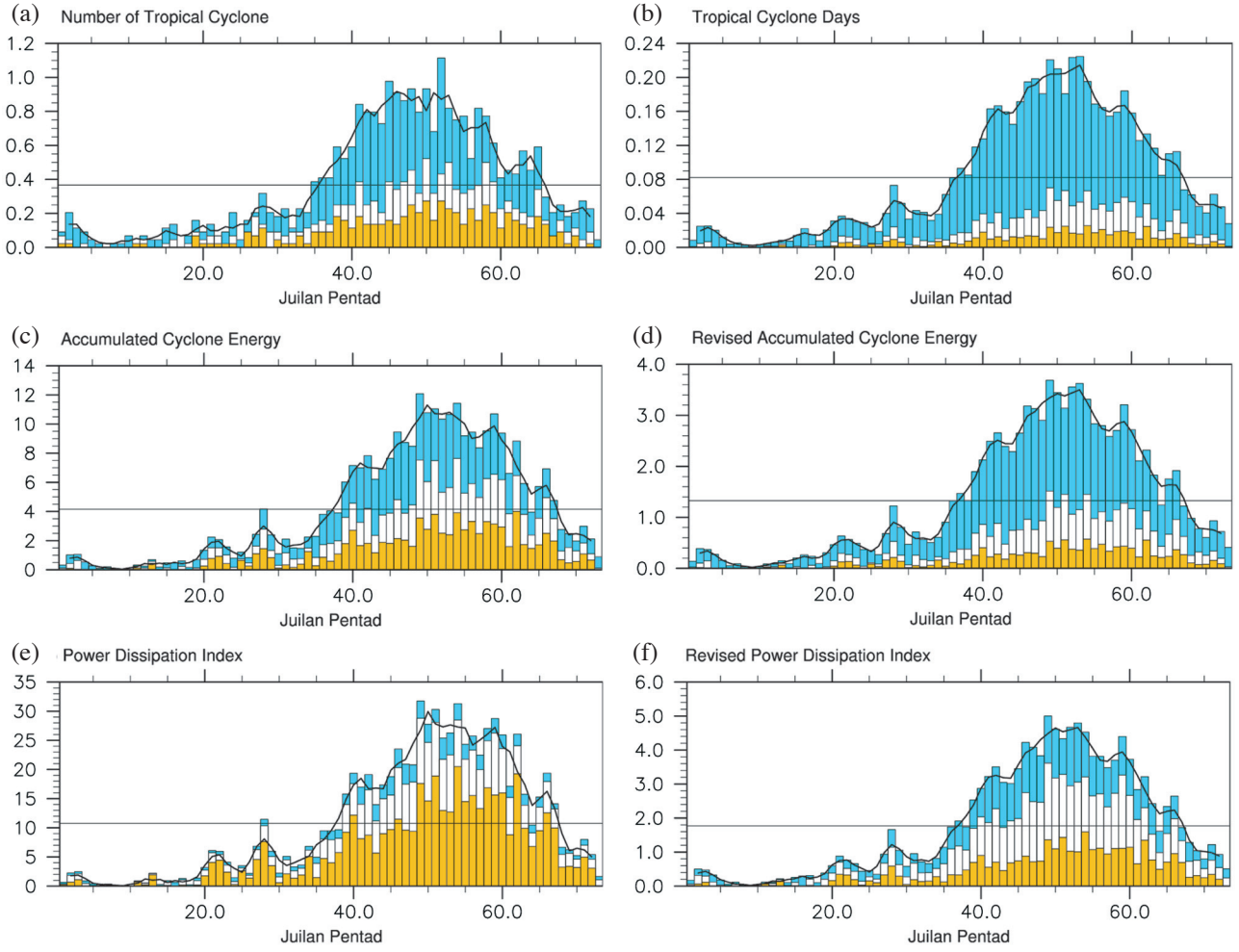

Fig. 3. Same as in Fig. 1, but showing the pentadly annual cycle of TC activity over the WNP. The relative contributions to TC activity from severe hurricanes, hurricanes, and tropical storms are displayed in yellow, white and cyan, respectively. The horizontal lines denote the mean values of respective metrics; while the curves denote the 15-day running-mean values to highlight the high-frequency fluctuation signals.

seasonal evolution patterns of TC activity with a finer temporal view. We also find that, in many respects, including seasonal cycle and relative partition of TC activity, a strong resemblance occurs among TCD, RACE and RPDI.

Table 1 summarizes the relative contribution (in percentage) to NTC, TCD, ACE, RACE, PDI and RPDI from severe hurricane, hurricane and tropical storm groups, respectively. As expected, the contribution from severe hurricanes seems to be largely overestimated in ACE (42%) and PDI (56%), as compared with the one in TCD (16%), RACE (22%) and RPDI (26%). It again confirms that the metrics using simple approximations of wind power (e.g., ACE and PDI) tend to put more weight on strong TC systems.

3.2 Spatial Distribution Pattern

Figure 4 displays the spatial patterns of NTC, TCD, ACE, RACE, PDI and RPDI evaluated at each 5° × 5° grid box over the WNP. For ease of comparison, the grid-box values are normalized by their respective maxima such that all values are within [0, 1]. For NTC (see Fig. 4a), two major formation regions of TC are observed: one located over the Philippine Sea around (10 ~ 20°N; 125 ~ 150°E); while the other located over the South China Sea around (10 ~ 20°N; 110 ~ 120°E). The TCD pattern (see Fig. 4b), however, manifests a very different picture, featuring a much more widespread TC activity pattern due to the inclusion of TC duration and intensity within and are consistent with the findings of Chen et al. (2006). The ACE pattern (see Fig. 4c), on the other hand, is very similar to PDI pattern (see Fig. 4e). But both show a slightly different picture from that of TCD, characterized by a more narrowly confined TC activity pattern adjacent to the Philippine Sea and a relatively weak TC activity over the South China Sea. Once again, a strong resemblance occurs among spatial patterns of RACE (see Fig. 4d), RPDI (see Fig. 4f) and TCD. As shown in Table 2, the greatest pattern similarity occurs between TCD and RACE as well as between RPDI and RACE both with $r^2 = 0.99$, followed by ACE and RACE with $r^2 = 0.94$; while the similarity between NTC and RACE seems modest with $r^2 = 0.42$.

4. CONTRAST IN CLIMATE VARIABILITY

In this section, anomaly patterns of NTC, TCD, ACE, RACE, PDI and RPDI associated with El Niño and La Niña events, along with their long-term trends over the past few decades, are compared. In climate studies, selections of El Niño (La Niña) years are often defined according to the Nino 3.4 index over the period of interest (Chen et al. 1998; Chan 2000). In this study, an El Niño (La Niña) year is referred to one in which the Nino 3.4 index is greater (smaller) than 0.5 (-0.5) during the JASON period. Based on the Nino 3.4 index data from the ENSO monitoring homepage of the Climate Prediction Center*, 11 El Niño years (1965, 72, 82, 86, 87, 91, 94, 97, 02, 04 and 06) and 9 La Niña years (1970, 71, 73, 74, 75, 85, 88, 98 and 99) can be identified.

4.1 El Niño and La Niña Years

Figure 5 shows the anomaly patterns of NTC, TCD, ACE, RACE, PDI and RPDI composited over the above 11 El Niño years. These anomaly patterns are derived by subtracting El Niño composite from the 1965 ~ 2008 climatology. As shown in Fig. 5, significant anomalies occur across almost the entire WNP for all metrics, including South China Sea. For NTC (see Fig. 5a), positive anomalies dominate the southeastern part of the WNP; while negative anomalies dictate the northwestern part. This implies that the major birthplace of TC would be shifted southeastward during an El Niño year (Chen et al. 1998; Chia and Ropelewski 2002; Chen et al. 2006). For TCD, ACE, RACE, PDI and RPDI anomalies (see Figs. 5b ~ f), a completely different picture appears, with positive anomalies dominating almost the entire WNP basin except over the South China Sea. This implies that the total TC activity (including intensity and duration of TC) would be significantly strengthened during an El Niño year (Wang and Chan 2002; Camargo and Sobel 2005). Moreover, as shown by positive anomalies of TCD, ACE, RACE, PDI and RPDI south of Japan, there is a tendency that Japan is likely to experience more TC impacts in El Niño years. For example, a record high of 10 typhoons making landfall on Japan was recorded in 2004, which is an extreme case of El Niño influence compared with the mean number of about 2.6 per year (Hitoshi et al. 2006).

Likewise, Fig. 6 shows the anomaly patterns of NTC, TCD, ACE, RACE, PDI and RPDI, composited over the 9 La Niña years. In general, the patterns shown in Fig. 6 are simply the reverse of those in Fig. 5. This implies that the major birthplace of a TC would be shifted northwestward during a La Niña year (see Fig. 6a). Meanwhile, spatial patterns of TCD, ACE, RACE, PDI and RPDI (see Figs. 6b ~ f) all suggest that the total TC activity would be significantly weakened during a La Niña year. Since changes of atmospheric circulation in La Niña years are in general opposite to those in El Niño years (Wu et al. 2004), the reversed TC activity patterns shown in Figs. 5 and 6 seem plausible. Also shown in Table 2, the greatest pattern similarity during El Niño (La Niña) years occurs between RPDI and RACE with $r^2 = 0.99$ (0.99), followed by TCD and RACE with $r^2 = 0.94$ (0.96). The similarity between ACE and RACE seems to be slightly lower with $r^2 = 0.89$ (0.87), followed by PDI and

* http://www.cpc.noaa.gov/products/analysis_monitoring/ensostuff/ensoyears.shtml.

Table 1. Relative contribution (in percentage) to annual magnitudes of NTC, TCD, ACE, RACE, PDI and RPDI from the severe hurricane ($v_{max} > 96$ knots), the hurricane ($64 \le v_{max} \le 95$ knots), and the tropical storm ($35 \le v_{max} \le 63$ knots) groups, respectively.

	NTC	TCD	ACE	RACE	PDI	RPDI
Severe Hurricane	33%	16%	42%	22%	56%	26%
Hurricane	30%	31%	36%	38%	32%	40%
Tropical Storm	37%	53%	22%	40%	12%	34%

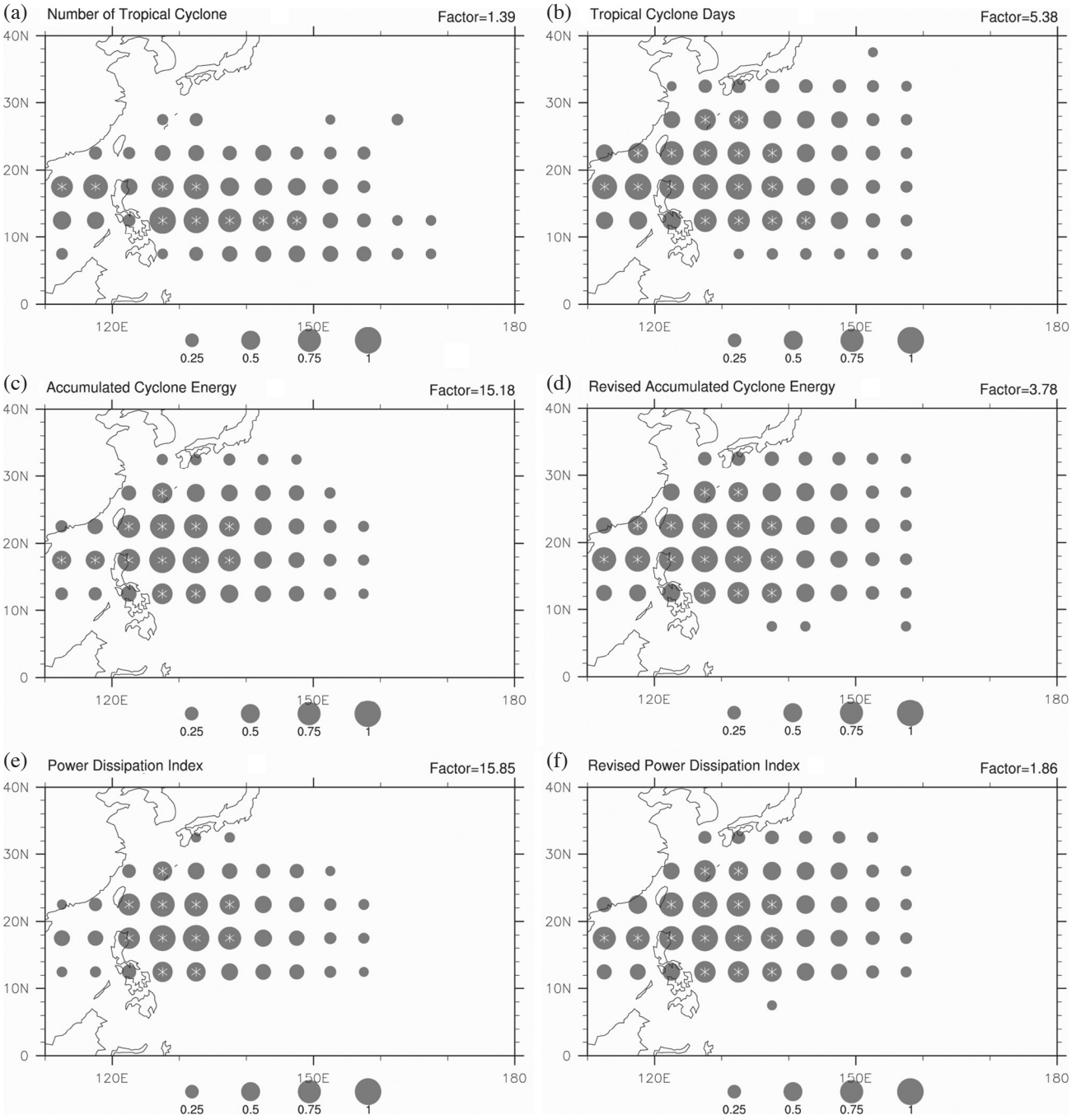

Fig. 4. Spatial distributions of NTC, TCD, ACE, RACE, PDI and RPDI evaluated at each 5° × 5° grid box over the WNP basin during the period 1965 ~ 2008. For ease of comparison, all grid-box values are rescaled such that they are within [0, 1]. Magnitudes over 0.5 are highlighted with the asterisks (∗) within the circles. The respective rescaling factors are displayed at the upper right corners.

Table 2. Pattern similarities between RACE and the remaining metrics associated with climatology (first row), El Niño (second row) and La Niña (third row) years, respectively. The pattern correlation coefficient, denoted by the R-square value, is calculated over the region (5 ~ 30°N; 110 ~ 170°E) where frequent TC activity occurs.

	NTC vs. RACE	TCD vs. RACE	ACE vs. RACE	PDI vs. RACE	RPDI vs. RACE
Climatology	0.42	0.99	0.94	0.86	0.99
El Niño Years	0.11	0.94	0.88	0.70	0.99
La Niña Years	0.16	0.96	0.87	0.76	0.99

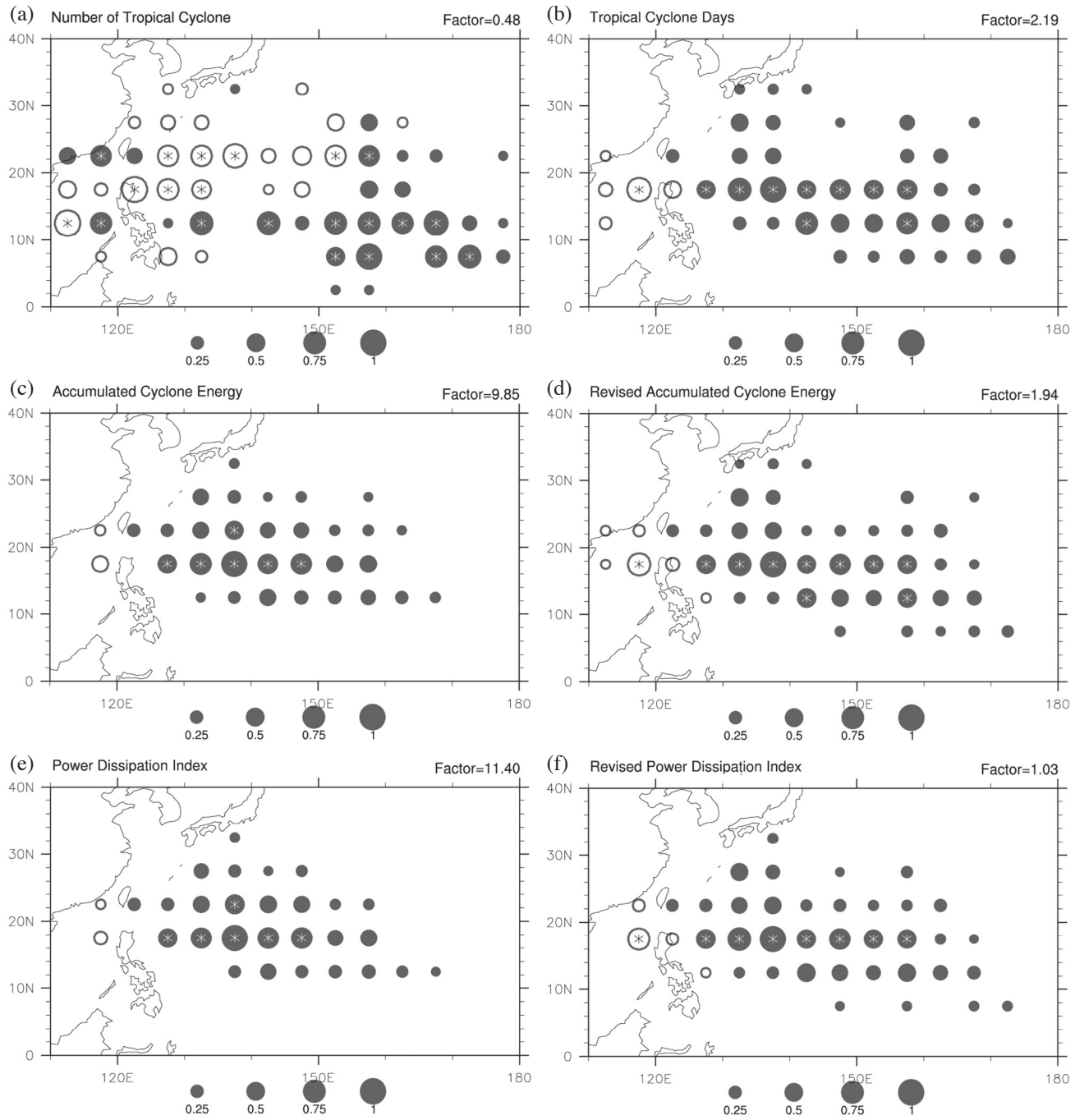

Fig. 5. Anomaly patterns of NTC, TCD, ACE, RACE, PDI and RPDI composited over the 11 El Niño years (1965, 72, 82, 86, 87, 91, 94, 97, 02, 04 and 06). All grid-box values are rescaled with magnitudes within [-1, 1]. Positive (negative) anomalies are denoted by solid (hollow) circles. Magnitudes over 0.5 are highlighted with the asterisks (⁎) within the circles. The respective rescaling factors are displayed at the upper right corners.

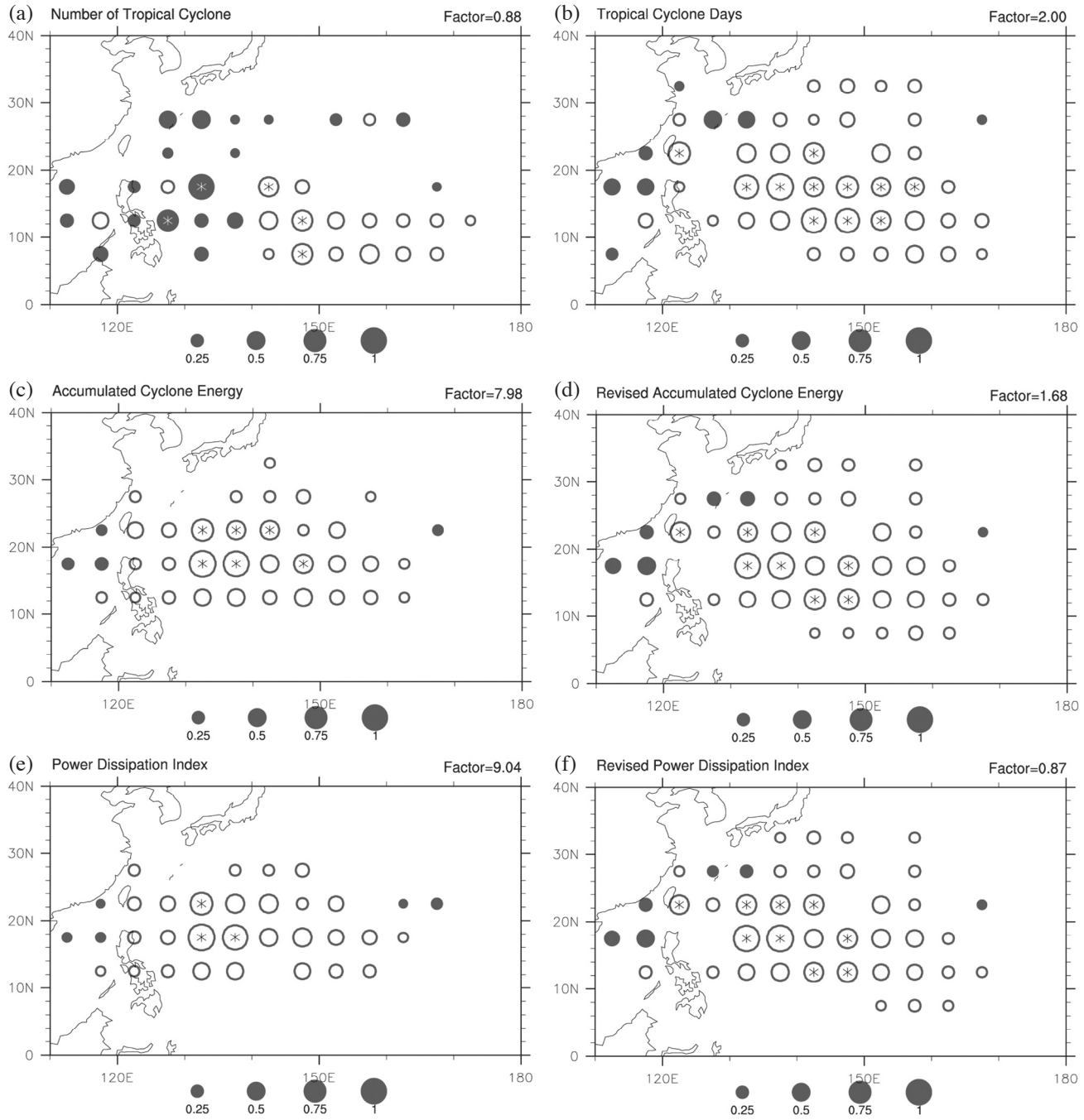

Fig. 6. Same as in Fig. 5, but for anomaly patterns of NTC, TCD, ACE, RACE, PDI and RPDI composited over the 9 La Niña years (1970, 71, 73, 74, 75, 85, 88, 98 and 99).

RACE with $r^2 = 0.70$ (0.76). Minimal similarity is observed between NTC and RACE with $r^2 = 0.11$ (0.16).

Furthermore, to highlight the magnitude changes of TC activity associated with El Niño and La Niña events, the mean magnitudes of NTC, TCD, ACE, RACE, PDI and RPDI averaged respectively over El Niño and La Niña years are summarized in Table 3. On average, about 26 TCs occur in a La Niña year, compared to about 28.5 TCs in an El Niño year. While the change in NTC seems very modest (≈10%), the changes in TCD, ACE, RACE, PDI and RPDI, nonetheless, are quite striking. For TCD, ACE, RACE, PDI and RPDI, the total TC activity would be strengthened by 56%, 95%, 64%, 120% and 70%, respectively, from a La Niña year to an El Niño year. These results clearly indicate that TC systems occurring in El Niño years are frequently stronger and longer-lived than those occurring in La Niña years and are consistent with Camargo and Sobel (2005) and Chen et al. (2006). The much larger changes in ACE

and PDI compared with TCD, RACE and RPDI are again due to overweighting of strong TC systems.

4.2 Long-Term Activity Trend

In Fig. 7, the long-term trends of annual NTC, TCD, ACE, RACE, PDI and RPDI over the last few decades are compared. As in Emanuel (2005), corrections to the raw JTWC maximum wind speed data prior to 1973 and a time smoother technique are applied beforehand. Also for ease of comparison, all metrics are rescaled to unity with respect to their respective magnitudes in 1973. Except for NTC, the remaining metrics have all shown an obvious upswing trend of TC activity since the early 1970s. Despite that most metrics have captured this upswing trend, the estimated magnitudes, however, are very diverse. For instance, when PDI has

Table 3. Mean magnitudes of NTC, TCD (in units of days), ACE (in units of 10^4 knot^2), RACE (in units of 10^4 knot^2), PDI (in units of 10^9 m^3 s^{-2}) and RPDI (in units of 10^9 m^3 s^{-2}) averaged respectively over the La Niña (first row) and El Niño (second row) years. To highlight their differences, the percentage changes from La Niña to El Niño years (third row) are displayed.

	NTC	TCD	ACE	RACE	PDI	RPDI
La Niña Years	26	2753	213	75	513	98.3
El Niño Years	28.5	4282	415	123	1128	167
Percentage Change	10%	56%	95%	64%	120%	70%

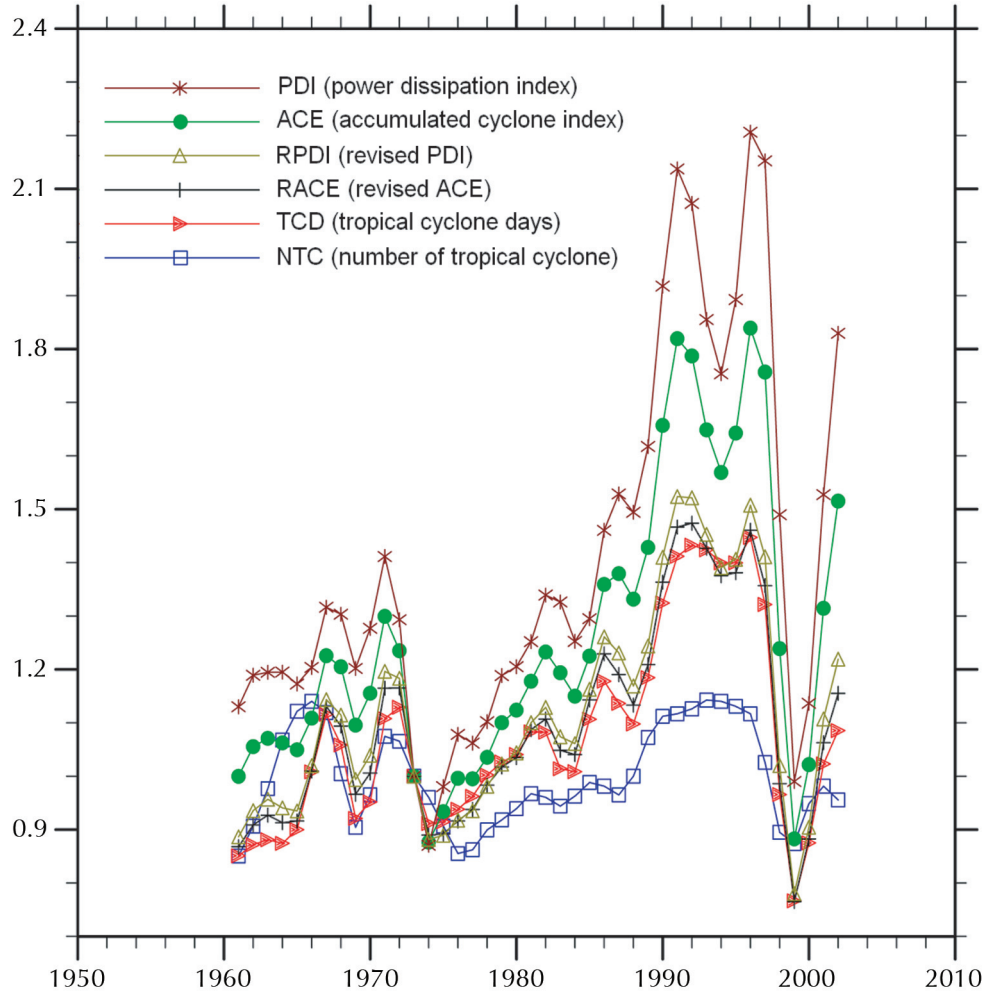

Fig. 7. Time series of NTC, TCD, ACE, RACE, PDI and RPDI derived from the JTWC best-track data over the WNP during the period 1960 ~ 2004. For ease of comparison, all metrics are rescaled to unity with respect to their respective magnitudes in 1973.

nearly doubled over the period from 1970 to 1997 (Emanuel 2005), RPDI only suggests an increase by only 45% or so. Likewise, when ACE has increased by nearly 70% over the same period, RACE only suggests an increase by only 43% or so. As compared with RPDI and RACE, the upswing trends of TC activity seem to be largely overestimated in PDI and ACE due to their simple approximations of wind power [see Eqs. (1) ~ (4) for comparison]. Another interesting feature shown in Fig. 7 is the striking resemblance between time series of RPDI, RACE and TCD regardless of very different approaches in estimating the total TC activity. This implies that the effects associated with various intensities of TC have been, to a certain extent, fairly considered within these metrics when a more precise estimation of the wind power is adopted.

Similar to Fig. 4, Fig. 8 shows the relative contributions to annual PDI and RPDI from various groups of TC systems. We find that, while both metrics show a similar fluctuation pattern, the partition pictures appear quite different. For PDI, the severe hurricane group accounts for the largest contribution (56%), followed by hurricane (32%) and tropical cyclone (12%) groups. For RPDI, on the other hand, all three TC groups seem to provide a relatively even partition picture (26%, 40%, and 34%, respectively). The overly weighted contribution from strong TC systems is apparently responsible for the much larger upswing trends of PDI (and ACE) as shown in Fig. 7.

5. CONCLUSION AND DISCUSSION

In this study, the metrics commonly used for measuring the total TC activity, including NTC, TCD, ACE, PDI, along with two newly proposed indices-RACE and RPDI, are compared using the JTWC best-track data of TC over the WNP basin, with an emphasis on their annual cycles, spatial distribution patterns, variability associated with El Niño and La Niña events, and long-term TC activity trends over the past few decades.

Analysis of the seasonal cycle pattern shows that, although most metrics seem to exhibit a similar seasonal transition pattern, some discrepancies can still be observed. Firstly, NTC reaches the peak in August; the remaining metrics (e.g., TCD, ACE, RACE, PDI and RPDI), nonetheless, all favor September to be the most frequent month for TC activity. It appears that the explicit inclusion of TC intensity and duration within the latter is responsible for such difference (Bell et al. 2000). Secondly, both ACE and PDI tend to exhibit greater magnitudes in the later period

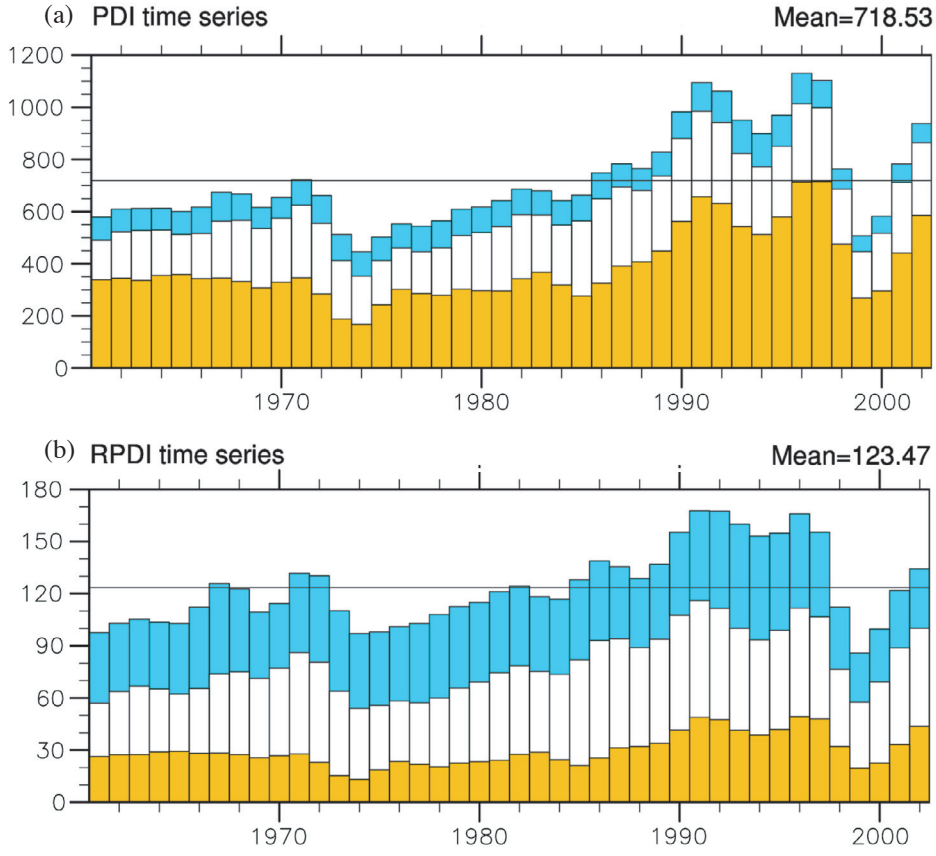

Fig. 8. Histograms showing the relative contributions to (a) PDI and (b) RPDI from the severe hurricane (in yellow), the hurricane (in white), and the tropical storm (in cyan) groups, respectively. The horizontal lines denote the mean values of the respective metrics.

of JASON (e.g., October and November), but TCD, RACE, and RPDI incline to have greater magnitudes in the earlier period (e.g., July and August). Such a feature can be attributed to more frequent occurrences of stronger TC systems in the later period of the TC season (see Fig. 2) because both ACE and PDI have a tendency to put more weight on strong TC systems compared with the other metrics (see Table 1).

Over the WNP, the TC activity is strongly controlled by El Niño and La Niña events. As shown by NTC anomalies over the WNP (see Figs. 5a and 6a), the major birthplace of TC systems would be shifted southeastward (northwestward) closer to the dateline (Asian continent) during an El Niño (a La Niña) year, despite only a modest change of NTC (see Table 3). The remaining metrics (e.g., TCD, ACE, RACE, PDI and RPDI), however, all indicate that the total TC activity would be significantly enhanced (weakened) during an El Niño (a La Niña) year primarily because of longer (shorter) TC lifetime and greater (smaller) TC intensity (see Table 3). Overall, the results presented in this study are qualitatively consistent with previous studies (Chen et al. 1998; Chia and Ropelewski 2002; Wang and Chan 2002; Chen et al. 2006).

Analysis of the long-term TC activity trends over the WNP further demonstrates that, while most metrics have captured the upswing trends of TC activity over the past few decades, the estimated magnitudes appear very diverse, depending on the metrics used for characterizing TC activity. As compared with TCD, RACE and RPDI, the upswing trends seem to be largely overestimated in PDI and ACE due to overly weighted contribution from strong TC systems (see Fig. 8). Our study also shows that, in many respects (e.g., seasonal cycle, variability associated with El Niño and La Niña years and long-term TC activity trend), a striking resemblance occurs among TCD, RACE and RPDI. Since RACE and RPDI consider the contribution to TC activity from various intensities on a fair basis (Yu et al. 2009), it is reasonably speculated that they should provide a more precise estimate of the TC activity trend compared with the remaining metrics. Because a stronger TC often lasts longer, as a result, TCD not only includes the duration, but also adds information on the intensity. This can explain why TCD, RACE and RPDI behave so similarly.

One major concern arising in this study broaches the question of whether there is a need to define a "universal" or "best" metric for TC activity. We argue that, while RACE and RPDI seem to provide a more precise estimate of the wind power compared with the conventional ACE and PDI, it dose not imply that the conventional metrics are inaccurate or inappropriate. In practical terms, different metrics are designed to stratify different aspects of TC activity. For example, NTC focuses on genesis number and location. TCD adds additional information on the lifetime of each individual TC, ACE and PDI, not only consider the number and duration, but also put additional weight on the intensity. On the other hand, RACE and RPDI can be viewed as improved versions of the conventional ones because no extra weight is added on strong TC systems.

To test the sensitivity of the above results to various data sources, two additional best-track data, including the Japan Meteorological Agency (JMA) best track and the international best track archive for climate stewardship (IBTrACS), are selected for comparison against the JTWC data (see Appendix B for a detailed description). In sum, except for magnitude change, the general patterns of TC activity are insensitive to the choice of datasets.

Acknowledgements This study was sponsored by the National Science Council of Taiwan under Grants NSC99-21 11-M-034-001 and NSC99-2111-M-034-003. The authors acknowledge the three anonymous reviewers for their constructive comments and helpful suggestions.

REFERENCES

Bell, G. D., M. S. Halpert, R. C. Schnell, R. W. Higgins, J. Lawrimore, V. E. Kousky, R. Tinker, W. Thiaw, M. Chelliah, and A. Artusa, 2000: Climate assessment for 1999. *Bull. Amer. Meteorol. Soc.*, **81**, 1328-1328, doi: 10.1175/1520-0477(2000)081<1328:CAF>2.3.CO;2. [Link]

Camargo, S. J. and A. H. Sobel, 2005: Western North Pacific tropical cyclone intensity and ENSO. *J. Climate*, **18**, 2996-3006, doi: 10.1175/JCLI3457.1. [Link]

Chan, J. C. L., 2000: Tropical cyclone activity over the western North Pacific associated with El Niño and La Niña events. *J. Climate*, **13**, 2960-2972, doi: 10.1175/1520-0442(2000)013<2960:TCAOTW>2.0.CO;2. [Link]

Chen, T. C., S. P. Weng, N. Yamazaki, and S. Kiehne, 1998: Interannual variation in the tropical cyclone formation over the western North Pacific. *Mon. Weather Rev.*, **126**, 1080-1090, doi: 10.1175/1520-0493(1998)126<1080:IVITTC>2.0.CO;2. [Link]

Chen, T. C., S. Y. Wang, and M. C. Yen, 2006: Interannual variation of the tropical cyclone activity over the western North Pacific. *J. Climate*, **19**, 5709-5720, doi: 10.1175/JCLI3934.1. [Link]

Chia, H. H. and C. F. Ropelewski, 2002: The interannual variability in the genesis location of tropical cyclones in the northwest Pacific. *J. Climate*, **15**, 2934-2944, doi: 10.1175/1520-0442(2002)015<2934:TIVITG>2.0.CO;2. [Link]

Emanuel, K., 2005: Increasing destructiveness of tropical cyclones over the past 30 years. *Nature*, **436**, 686-688, doi: 10.1038/nature03906. [Link]

Emanuel, K., 2006: Climate and tropical cyclone activity: A new model downscaling approach. *J. Climate*, **19**, 4797-4802, doi: 10.1175/JCLI3908.1. [Link]

Emanuel, K., 2007: Environmental factors affecting tropical cyclone power dissipation. *J. Climate*, **20**, 5497-5509, doi: 10.1175/2007JCLI1571.1. [Link]

Goldenberg, S. B., C. W. Landsea, A. M. Mestas-Nuñez, and W. M. Gray, 2001: The recent increase in Atlantic Hurricane activity: Causes and implications. *Science*, **293**, 474-479, doi: 10.1126/science.1060040. [Link]

Henderson-Sellers, A., H. Zhang, G. Berz, K. Emanuel, W. Gray, C. Landsea, G. Holland, J. Lighthill, S. L. Shieh, P. Webster, and K. McGuffie, 1998: Tropical cyclones and global climate change: A post-IPCC assessment. *Bull. Amer. Meteorol. Soc.*, **79**, 19-38, doi: 10.1175/1520-0477(1998)079<0019:TCAGCC>2.0.CO;2. [Link]

Hitoshi, S., B. Kotaro, N. Tetsuo, U. Mitsuru, W. Akiyoshi, H. Shunsuke, T. Hiroo, K. Masaru, K. Naoko, M. Akihiko, and M. Wataru, 2006: Summary of landfalling typhoons in Japan, 2004 by Typhoon Research Department, Technical Reports of the Meteorological Research Institute, 44 pp.

Ho, C. H., J. J. Baik, J. H. Kim, D. Y. Gong, and C. H. Sui, 2004: Interdecadal changes in summertime typhoon tracks. *J. Climate*, **17**, 1767-1776, doi: 10.1175/1520-0442(2004)017<1767:ICISTT>2.0.CO;2. [Link]

Holland, G. J. and P. J. Webster, 2007: Heightened tropical cyclone activity in the North Atlantic: Natural variability or climate trend? *Phil. Trans. R. Soc. A*, **365**, 2695-2716, doi: 10.1098/rsta.2007.2083. [Link]

Knutson, T. R. and R. E. Tuleya, 2004: Impact of CO_2-induced warming on simulated hurricane intensity and precipitation: Sensitivity to the choice of climate model and convective parameterization. *J. Climate*, **17**, 3477-3495, doi: 10.1175/1520-0442(2004)017<3477:IOCWOS>2.0.CO;2. [Link]

Krayer, W. R. and R. D. Marshall, 1992: Gust factors applied to hurricane winds. *Bull. Amer. Meteorol. Soc.*, **73**, 613-618, doi: 10.1175/1520-0477(1992)073<0613:GFATHW>2.0.CO;2. [Link]

Landsea, C. W., N. Nicholls, W. M. Gray, and L. A. Avila, 1996: Downward trends in the frequency of intense at Atlantic hurricanes during the past five decades. *Geophys. Res. Lett.*, **23**, 1697-1700, doi: 10.1029/96GL01029. [Link]

Mallen, K. J., M. T. Montgomery, and B. Wang, 2005: Re-examining the near-core radial structure of the tropical cyclone primary circulation: Implications for vortex resiliency. *J. Atmos. Sci.*, **62**, 408-425, doi: 10.1175/JAS-3377.1. [Link]

Matthews, A. J., 2000: Propagation mechanisms for the Madden-Julian Oscillation. *Q. J. R. Meteorol. Soc.*, **126**, 2637-2651, doi: 10.1002/qj.49712656902. [Link]

Saunders, M. A. and A. R. Harris, 1997: Statistical evidence links exceptional 1995 Atlantic hurricane season to record sea warming. *Geophys. Res. Lett.*, **24**, 1255-1258, doi: 10.1029/97GL01164. [Link]

Sugi, M., A. Noda, and N. Sato, 2002: Influence of the global warming on tropical cyclone climatology: An experiment with the JMA global model. *J. Meteorol. Soc. Jpn.*, **80**, 249-272, doi: 10.2151/jmsj.80.249. [Link]

Wang, B. and J. C. L. Chan, 2002: How strong ENSO events affect tropical storm activity over the western North Pacific. *J. Climate*, **15**, 1643-1658, doi: 10.1175/1520-0442(2002)015<1643:HSEEAT>2.0.CO;2. [Link]

Waple, A. M., J. H. Lawrimore, M. S. Halpert, G. D. Bell, W. Higgins, and B. Lyon, 2002: Climate assessment for 2001. *Bull. Amer. Meteorol. Soc.*, **83**, 938-938, doi: 10.1175/1520-0477(2002)083<0938:CAF>2.3.CO;2. [Link]

Weatherford, C. L. and W. M. Gray, 1988a: Typhoon structure as revealed by aircraft reconnaissance. Part I: Data analysis and climatology. *Mon. Weather Rev.*, **116**, 1032-1043, doi: 10.1175/1520-0493(1988)116<1032:TSARBA>2.0.CO;2. [Link]

Weatherford, C. L. and W. M. Gray, 1988b: Typhoon structure as revealed by aircraft reconnaissance. Part II: Structural variability. *Mon. Weather Rev.*, **116**, 1044-1056, doi: 10.1175/1520-0493(1988)116<1044:TSARBA>2.0.CO;2. [Link]

Webster, P. J., G. J. Holland, J. A. Curry, and H. R. Chang, 2005: Changes in tropical cyclone number, duration, and intensity in a warming environment. *Science*, **309**, 1844-1846, doi: 10.1126/science.1116448. [Link]

Wu, M. C., W. L. Chang, and W. M. Leung, 2004: Impacts of El Niño - Southern Oscillation events on tropical cyclone landfalling activity in the western North Pacific. *J. Climate*, **17**, 1419-1428, doi: 10.1175/1520-0442(2004)017<1419:IOENOE>2.0.CO;2. [Link]

Yu, J. Y., C. Chou, and P. G. Chiu, 2009: A revised accumulated cyclone energy index. *Geophys. Res. Lett.*, **36**, L14710, doi: 10.1029/2009GL039254. [Link]

Yumoto, M. and T. Matsuura, 2001: Interdecadal variability of tropical cyclone activity in the western north Pacific. *J. Meteorol. Soc. Jpn.*, **79**, 23-35, doi: 10.2151/jmsj.79.23. [Link]

APPENDIX A: MATHEMATICAL DERIVATION FOR RPDI

To provide a more precise estimate of Emanuel's (2005) PDI, we consider a modified Rankine vortex wind structure similar to the RACE index (Yu et al. 2009):

$$v(r)=\begin{cases} v_{\max}\left(r/r_{\max}\right), & r \le r_{\max} \\ v_{\max}\left(r/r_{\max}\right)^{-\alpha}, & r > r_{\max} \end{cases} \tag{A1}$$

where r denotes the distance from the center of vortex, $v(r)$ represents the tangential wind, $r_{\max}$ is the radius of maximum tangential wind, and α depicts the decaying tendency

of wind outside r_{max}. The power dissipation can thus be re-written as

$$P(r) = \begin{cases} v_{max}^3 (r/r_{max})^3 , & r \le r_{max} \\ v_{max}^3 (r/r_{max})^{-3\alpha} , & r > r_{max} \end{cases} \quad \text{(A2)}$$

A non-dimensional form of Eq. (A2) gives

$$\tilde{P}(\tilde{r}) = \begin{cases} \tilde{r}^3 , & \tilde{r} \le 1 \\ \tilde{r}^{-3\alpha} , & \tilde{r} > 1 \end{cases} \quad \text{(A3)}$$

where the tilde variables (unitless quantities) are defined as below:

$$\tilde{r} = r/r_{max}, \quad \tilde{P} = P/P_{max}, \quad P_{max} = v_{max}^3 \quad \text{(A4)}$$

We note that P_{max} in Eq. (A4) denotes the original definition of power dissipation as in Emanuel (2005).

Integrating Eq. (A3) over a circular area within a certain radius and dividing it by the same area, we obtain an area mean value of the power dissipation:

$$\tilde{P} = \frac{1}{\pi \tilde{r}_c^2} \int_0^{\tilde{r}_c} \int_0^{2\pi} \tilde{P}(\tilde{r}) \cdot \tilde{r} \, d\theta \, d\tilde{r} = \frac{1}{\tilde{r}_c^2} \left[\frac{2}{5} + \frac{2\tilde{r}_c^{(2-3\alpha)} - 2}{(2 - 3\alpha)} \right] \quad \text{(A5)}$$

where $\tilde{r}_c$ denotes the cut-off radius (unitless) within which the power dissipation associated with a TC is estimated. The first and second terms in the bracket of Eq. (A6) represent the contribution to power dissipation from circulations within and outside r_{max}, respectively.

The dimensional form of Eq. (A5) yields

$$P = \frac{v_{max}^3}{\tilde{r}_c^2} \left[\frac{2}{5} + \frac{2\tilde{r}_c^{(2-3\alpha)} - 2}{(2 - 3\alpha)} \right] \quad \text{(A6)}$$

The revised power dissipation index (RPDI) is defined by summing up the 6-hourly TC records using Eq. (A6). As far as the mean power dissipation is concerned, $\tilde{P}$ in Eq. (A5) denotes a rescaling factor of the conventional PDI.

Figure A1 shows the difference between PDI and RPDI as a function of v_{max}. For convenience, only their non-dimensional counterparts are displayed. In general, magnitudes of RPDI are much smaller than those of PDI. The difference between PDI and RPDI enlarges as the TC intensity (x_{max}) increases. For example, RPDI is about 40% the size of PDI at tropical storm intensity ($34 \le v_{max} \le 63$ knots), and this ratio decreases quickly to 20% at hurricane intensity ($64 \le v_{max} \le 95$ knots) and 10% at severe hurricane intensity ($v_{max} > 96$ knots). This implies that PDI has a great potential to overestimate the TC activity especially for strong TC systems.

APPENDIX B: SENSITIVITY TO DATA SOURCE

In addition to the JTWC best track data, several meteorological agencies (e.g., the Japan Meteorological Agency, National Oceanic and Atmospheric Administration, Hong Kong Observatory, and China Meteorological Administration) also generated best track data of TCs over the WNP basin. To test the sensitivity of our study to various data sources, two other popular datasets were selected for comparison using ACE as the target metric. The two best-track datasets used here included the Japan meteorological Agency (JMA) best track data from 1977 to 2008 and the international best track archive for climate stewardship (IBTrACS) from 1965 to 2008. Unlike the JTWC data that utilized one-minute average wind speed for v_{max} (i.e., the maximum sustained wind speed), both JMA and IBTrACS data used 10-minute average. As shown in Krayer and Marshall (1992), the two definitions were highly correlated, with the former conventionally about 14% higher than the latter.

Figure B1 shows the annual cycle, climatic spatial distribution, the El Niño anomaly and La Niña anomaly patterns of ACE derived respectively from JMA and IBTrACS data. We found that, except for magnitude difference, all aspects of TC activity obtained from JMA and IBTrACS data, including seasonal cycle (Figs. B1a and b), spatial distribution pattern (Figs. B1c and d) and anomalies associated with El Niño (Figs. B1e and f) and La Niña events (Figs. B1g and h), are very similar to those obtained from JTWC data (Figs. 1c, 4c, 5c, and 6c). It is found that changes in ACE magnitude result mostly from different definitions of v_{max}. On average, definition of v_{max} based on one-minute average wind speed (e.g., the JTWC data) would produce an annual ACE index approximately 25 to 30% larger than the one based on 10-minite average value (e.g., the JMA and IBTrACS data), quantitatively consistent with the findings of Krayer and Marshall (1992).

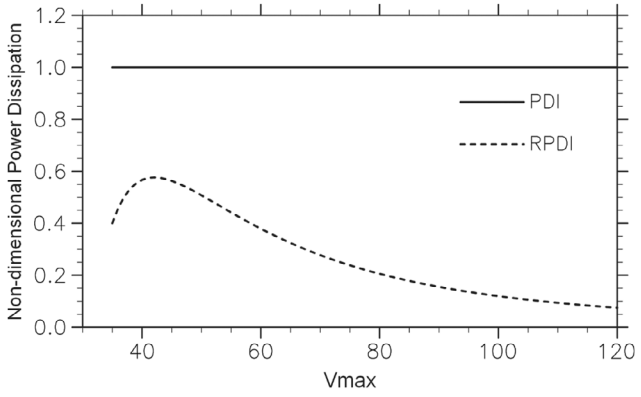

Fig. A1. Non-dimensional magnitudes of PDI (solid line) and RPDI (dash curve) as a function of the maximum sustained wind speed v_{max} (in knots).

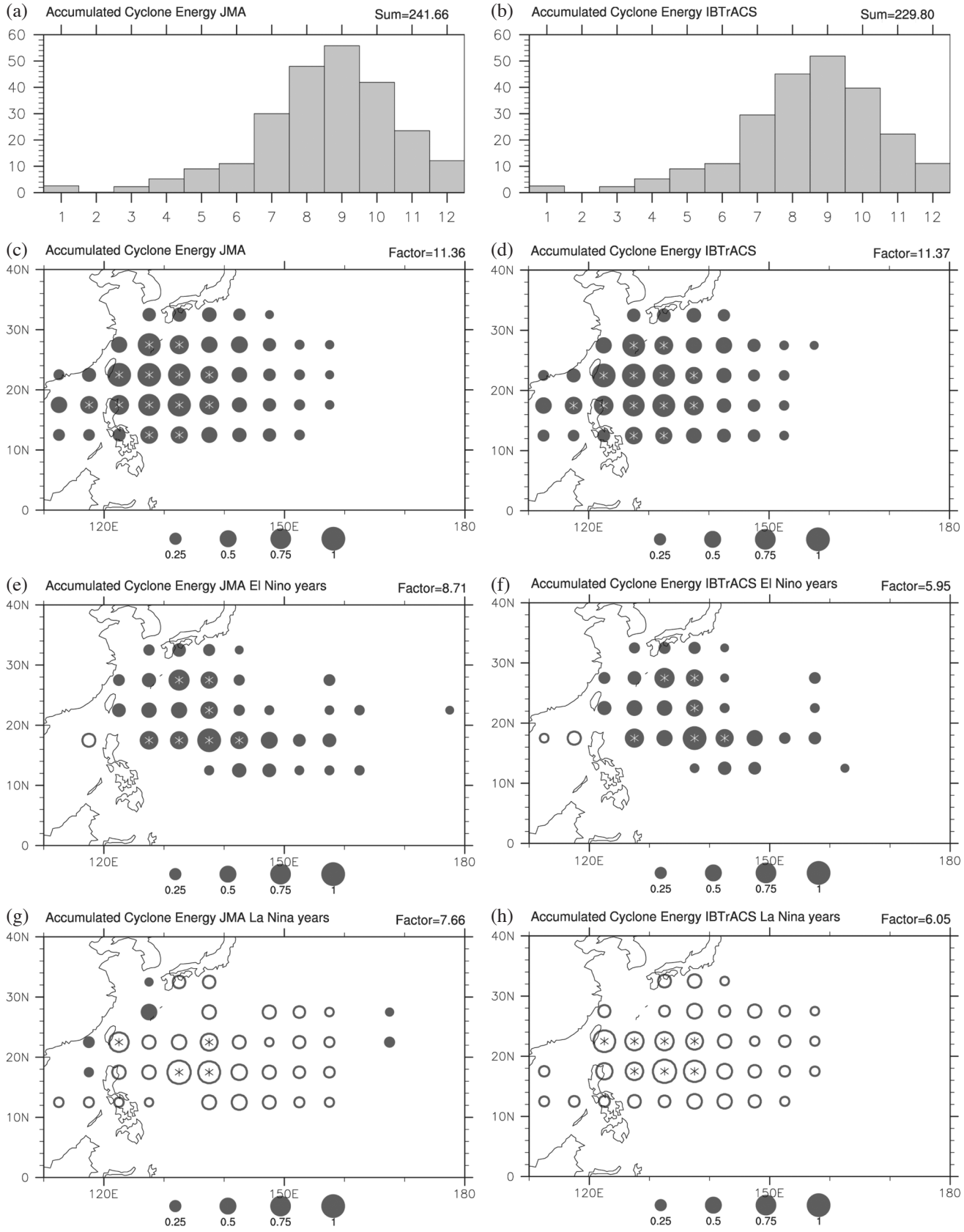

Fig. B1. From top to bottom: (a) (b) the seasonal cycle, (c) (d) the climatic distribution, (e) (f) the El Niño anomaly pattern, and (g) (h) the La Niña anomaly pattern of ACE derived from the JMA (left panels) and the IBTrACs (right panels) data, respectively. The JMA data used here covers a slightly shorter period (1977 ~ 2008) compared with the IBTrACs data (1965 ~ 2008). Notations used here are the same as in Figs. 1, 4, 5, and 6.